Thin Solid Films 754 (2022) 139300

Contents lists available at ScienceDirect

Thin Solid Films

journal homepage: www.elsevier.com/locate/tsf

Phase composition and magnetic properties of post-annealed asymmetric Pt/Fe/Pt/Au/Fe thin films

I.A. Vladymyrskyi [a,*], Y. Mamchur [a], O.V. Dubikovskyi [a,b], S.M. Voloshko [a], A. Ullrich [c], M. Albrecht [c]

[a] Paton Institute of Material Science and Electric Welding, National Technical University of Ukraine "Igor Sikorsky Kyiv Polytechnic Institute", Prospect Peremogy 37, 03056, Kyiv, Ukraine
[b] Department of Ion Beam Engineering, V.Ye. Lashkaryov Institute of Semiconductor Physics, NAS of Ukraine, Prospect Nauky 41, 03028 Kyiv, Ukraine
[c] Institute of Physics, University of Augsburg, Universitätsstraße 1, D-86159 Augsburg, Germany

ARTICLE INFO

Keywords:
Diffusion intermixing
Magnetic thin films
Iron-platinum alloys
Chemical $L1_0$ ordering

ABSTRACT

Intermetallic compound formation realized via thermally-induced diffusion intermixing of layered stacks is a prospective route for the formation of thin films with properties promising for practical applications. This can be further promoted by the addition of third elements which could provide acceleration of diffusion and ordering processes during post-annealing. In the present study, we have investigated the structural and magnetic properties of post-annealed Pt/Fe/Pt/Au/Fe thin films which contain an additional asymmetric Au layer and compare the results with Fe/Pt bilayers. It was shown that the introduction of an Au layer reduces both the onset temperature and the annealing time for promoting the formation the hard magnetic $L1_0$-FePt phase while the remaining layer stack develops a magnetically soft Pt-rich disordered FePt solid solution. Thus, different diffusion pathways present in asymmetric layer stacks can provide an intriguing root for thin film materials synthesis of exchange coupled soft and hard magnetic phases which could be of particular interest for the creation of graded magnetic nanomaterials.

1. Introduction

Thin films consisting of the chemically ordered $L1_0$-FePt phase have attracted a lot of attention in particular for applications in ultrahigh density heat assisted magnetic recording [1,2] and spintronics [3]. The significant practical potential of these films is caused by the unique properties of the $L1_0$-FePt phase including large magnetocrystalline anisotropy and coercive fields [4], high saturation magnetization [5] and Curie temperature [6] as well as excellent corrosion resistance [7].

One of the prospective approaches to form $L1_0$-FePt thin films is the deposition of Pt/Fe layer stacks followed by post-annealing. Annealing leads to thermally-induced interdiffusion processes between the layers forming first the disordered $A1$-FePt phase with subsequent chemical ordering [8,9]. Furthermore, the structural and magnetic properties of FePt thin films can be further modified by addition of third elements. For instance, Feng et al. [10] investigated the impact of Ag, Ti, and Bi additions introduced as underlayers to Pt/Fe multilayer samples after post-annealing. They found an enhancement of the coercivity which is most pronounced with Bi addition. Recently, Kruhlov et al. studied the sequence of thermally-induced structural phase transitions in Pt/Fe bilayers including additional layers of Mn [11] and Tb [12]. Furthermore, the addition of Au to FePt has been intensively studied. For instance, Ogata et al. [13] reported the formation of $L1_0$-FePt thin films by annealing of Fe/Pt/Au stacks, containing Au as a top layer. First, a homogeneous distribution of all three elements through the film depth was found after annealing at 500°C. However, further increase of the annealing temperature up to 600°C leads to an inhomogeneous distribution of Au with the existence of clear segregation regions at the free surface and film/substrate interface. Limited solubility of Au in Fe, Pt, and FePt alloy suggests a dominated grain boundary diffusion mechanism.

Generally, the addition of Au layers to Fe/Pt layer stacks provides a reduction in $L1_0$-FePt phase formation temperature and a significant enhancement of the coercive field [14,15] compared to annealed Fe/Pt bilayers which depends strongly on the initial Au layer thickness. The latter is achieved by strong magnetic decoupling of the hard magnetic FePt grains by the formation of grain boundaries saturated by Au [15]. Thus, variation of the thickness of the Au layer in Pt/Fe-based stacks and

* Corresponding author at: Prospect Peremogy 37, 03056, Kyiv, Ukraine.
E-mail address: vladymyrskyi@kpm.kpi.ua (I.A. Vladymyrskyi).

https://doi.org/10.1016/j.tsf.2022.139300
Received 29 November 2021; Received in revised form 12 April 2022; Accepted 10 May 2022
Available online 18 May 2022

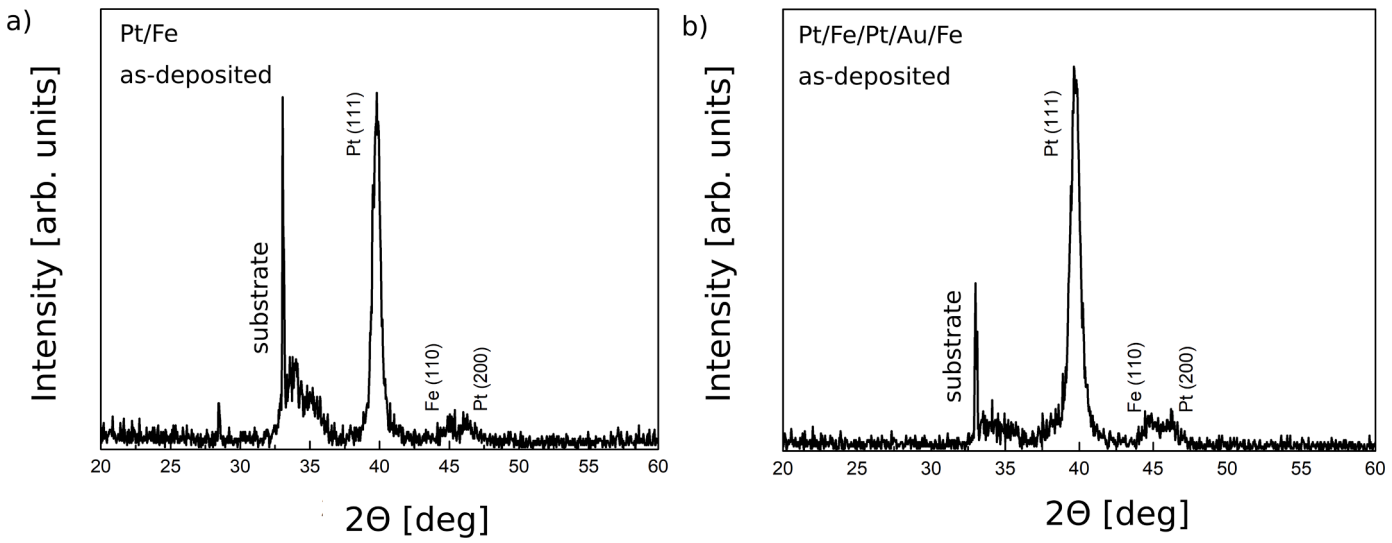

Fig. 1. XRD (θ–2θ) scans of (a) Pt/Fe and (b) Pt/Fe/Pt/Au/Fe films after deposition.

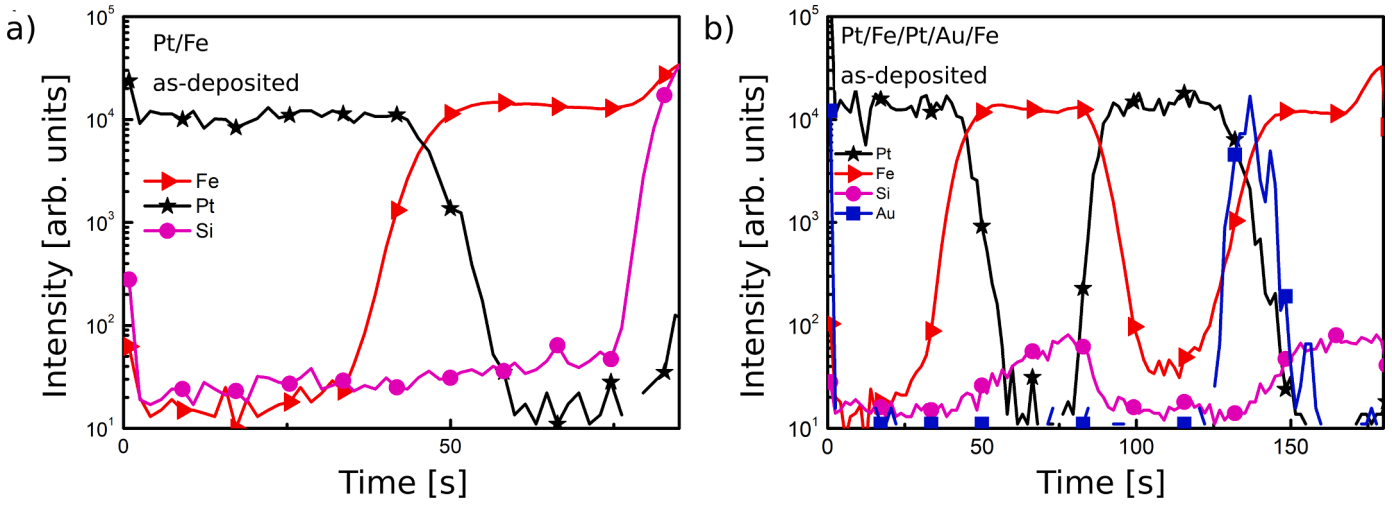

Fig. 2. SIMS chemical depth profiles of (a) Pt/Fe and (b) Pt/Fe/Pt/Au/Fe films after deposition (Pt and Au intensities were artificially increased up to the Fe level for better visibility).

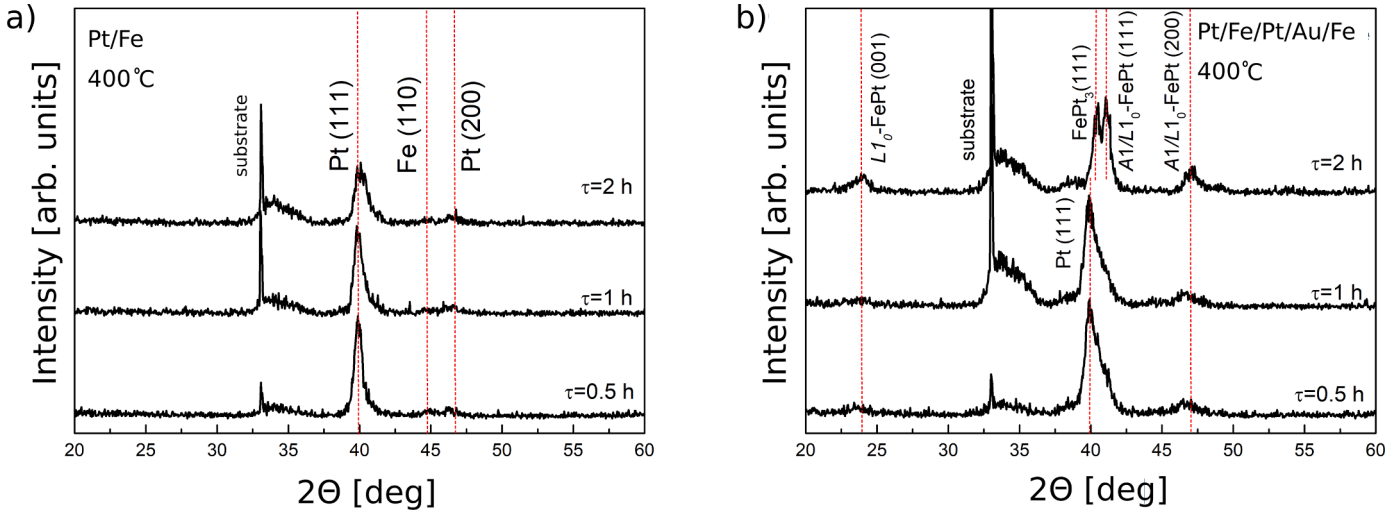

Fig. 3. XRD (θ–2θ) scans of (a) Pt/Fe and (b) Pt/Fe/Pt/Au/Fe films annealed at 400°C for different annealing times.

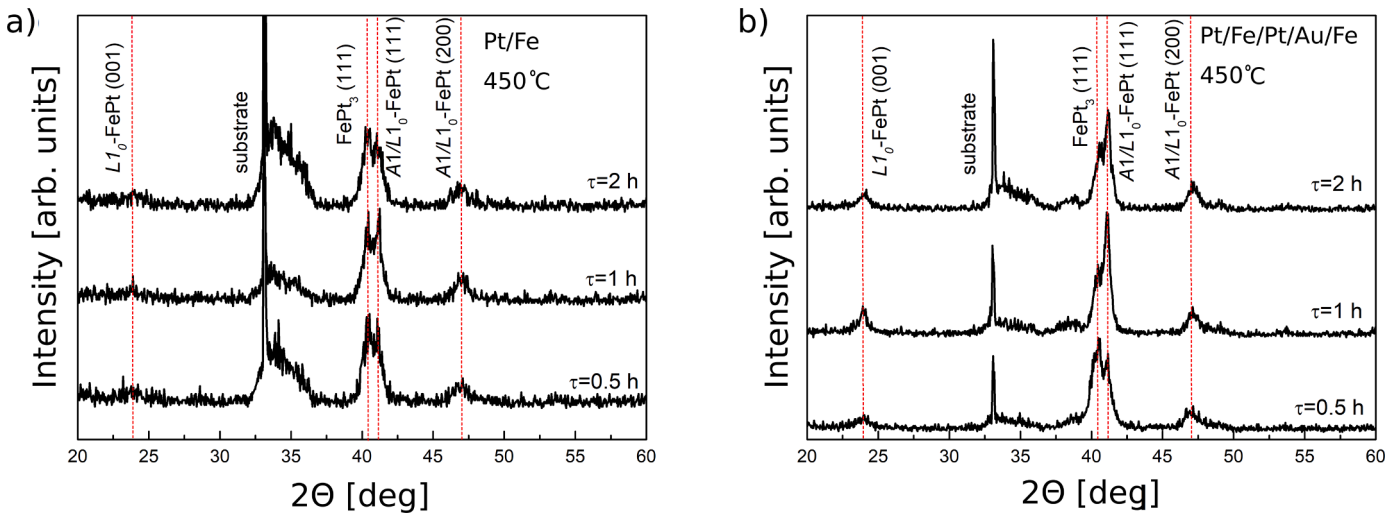

Fig. 4. XRD (θ–2θ) scans of (a) Pt/Fe and (b) Pt/Fe/Pt/Au/Fe films annealed at 450°C for different annealing times.

control of post-annealing parameters allow varying the kinetics of the chemical ordering process and, as a consequence, the fraction of the disordered *A*1-FePt and ordered $L1_0$-FePt phase in the film. Coexistence of these two phases reveals practical interest in case of deposition and post-annealing of the Fe/Pt stacks with asymmetrical position of the Au layer. In this case, diffusion and phase formation could be facilitated in one part of the stack, leading to an inhomogeneous distribution of soft and hard magnetic phases through the depth of the films which could be of interest for the creation of FePt-based graded magnetic media [16–20].

In the present study, we report on the structure and magnetic properties of post-annealed asymmetric Pt/Fe/Pt/Au/Fe thin films. Heat treatment was carried out under various annealing temperatures and annealing times in order to induce diffusion intermixing between the layers and to promote structural phase transitions in the film material, and compare these properties with post-annealed Pt/Fe bilayers.

2. Experimental details

Pt(15.7 nm)/Fe(12 nm)/sub. and Pt(15.7 nm)/Fe(12 nm)/Pt(15.7 nm)/Au(6 nm)/Fe(12 nm)/sub. films were prepared by direct current (DC) magnetron sputtering at room temperature on single crystal Si (100) substrates with a 100 nm-thick amorphous SiO_2 layer using individual Fe, Pt, and Au targets. The layer thicknesses of Pt and Fe were chosen to provide an equiatomic Fe/Pt ratio in case a fully homogenous FePt alloy is formed after post-annealing. Depositions were performed in a BESTEC UHV sputter system (base pressure of $<5\times10^{-6}$ Pa) using an Ar sputter gas pressure of 0.5 Pa. The sputtering rates and film thicknesses of each layer were adjusted by a calibrated quartz crystal microbalance before each deposition. The following sputter powers and deposition rates were applied: 58 W / 0.17 A/s for Fe, 41 W / 0.42 A/s for Pt, and 33 W / 1.00 A/s for Au. As-deposited films were post-annealed in the temperature range between 350 °C and 450 °C in a separate vacuum chamber (10^{-3} Pa) using a heating rate of 0.5 °C/s. After reaching the final temperature, the samples were further annealed from 0.5 up to 2 hours (h).

Phase composition of the samples was analyzed at room temperature by x-ray diffraction (XRD, Rigaku Ultima IV diffractometer) in (θ-2θ) geometry using Cu-Kα radiation. For a detailed structural characterization of the interfaces and elemental distribution of the layer stacks, high-angle annular dark-field scanning transmission electron microscopy (HAADF STEM) imaging and spectrum imaging analysis based on energy-dispersive x-ray spectroscopy (EDS) were performed utilizing a JEOL NEOARM200F instrument with an operating voltage of 200 kV. Classical cross-sectional TEM samples were prepared by sawing, grinding, polishing, mechanical dimpling, and final Ar-ion milling. This study was supported by secondary ions mass spectrometry (SIMS) depth profiling, using an Ion Tof IV system. Positive O+ ions with an energy of 1 keV using a current of 250 nA were applied for layer sputtering, while Bi+ ions (25 keV, 1.5 pA) were used to induce emission of secondary ions to be detected by mass spectrometry. The magnetic properties of the samples were investigated using superconducting quantum interference device-vibrating sample magnetometry (SQUID-VSM, MPMS3, LOT-QuantumDesign GmbH).

3. Results and discussion

Fig. 1 shows XRD (θ-2θ) patterns of the Pt/Fe and Pt/Fe/Pt/Au/Fe film samples in the as-deposited state. For both samples, a well pronounced Pt(111) peak and weak Fe(110) and Pt(200) reflections can be detected. SIMS chemical depth profiles of the as-deposited films are presented in Fig. 2, revealing the expected layer stacking. Please note, that Pt, Fe, and Au sputtered from the corresponding separate layers of the as-deposited stacks reveal different intensities caused by different work functions of these elements. Thus, the intensities of Pt and Au were artificially increased up to the Fe level to improve the clarity. We believe that the detected overlap of the signals between the metallic layers in the as-deposited stacks is mainly caused by chemical roughness and intermixing at the interfaces introduced during the growth process as well as during the SIMS sputter process, which does not allow for a quantitative analysis.

Post-heat treatment of the as-deposited samples was carried out

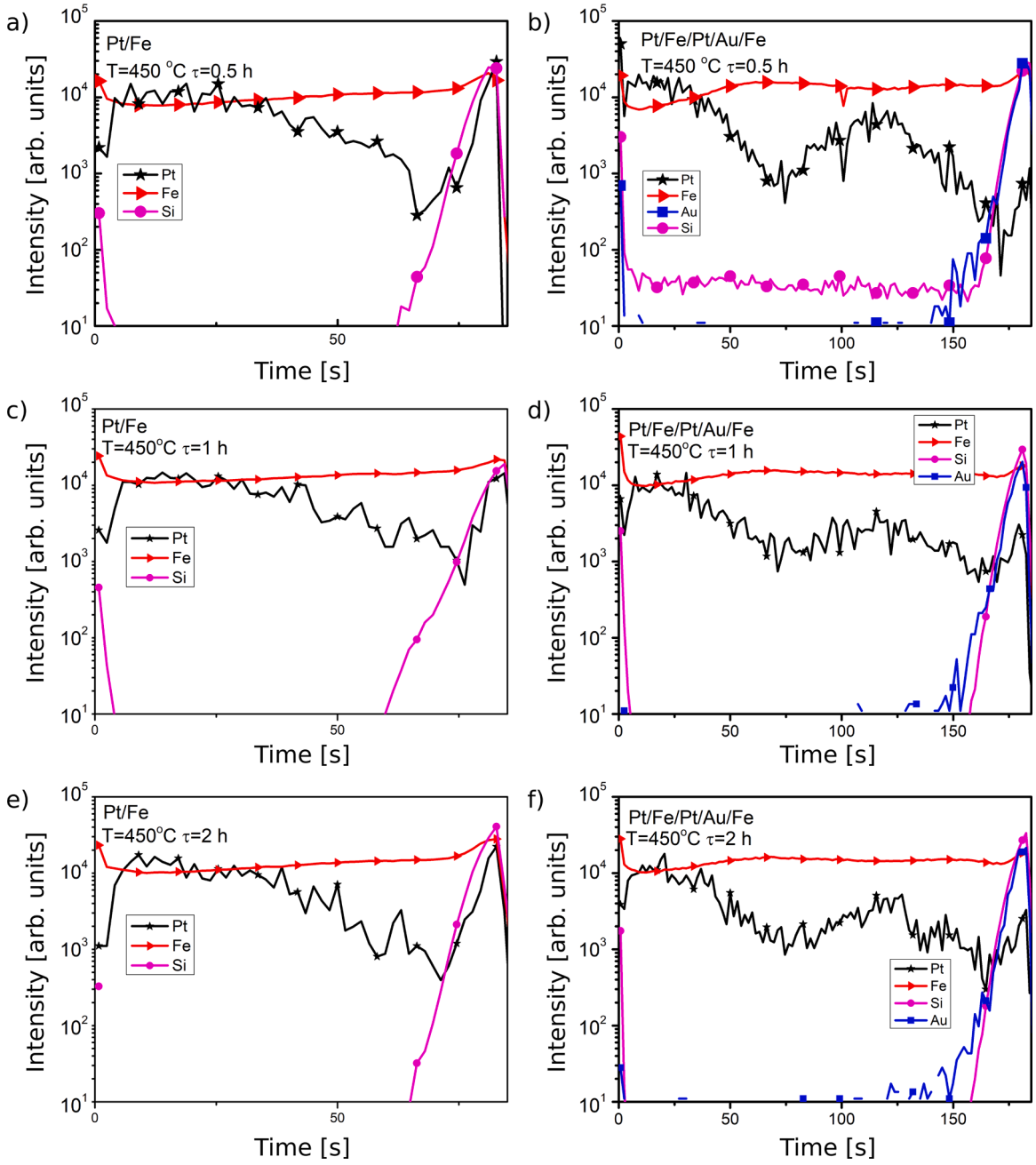

Fig. 5. SIMS chemical depth profiles of (a,c,e) Pt/Fe and (b,d,f) Pt/Fe/Pt/Au/Fe films annealed at 450°C for (a,b) 0.5 h, (c,d)1 h, and (e,f) 2 h (Pt and Au intensities were artificially increased up to the Fe level for better visibility).

under various temperatures and annealing times in order to induce diffusion intermixing between the layers and to promote structural phase transitions in the film material. XRD (θ-2θ) patterns of the Pt/Fe and Pt/Fe/Pt/Au/Fe samples after post-annealing at 400 °C for different annealing times up to 2 h are displayed in Fig. 3. While the XRD patterns of the Pt/Fe bilayer after annealing at 400 °C for 0.5 h and 1 h are almost identical to the as-deposited sample, after 2 h of annealing a broadening of the Pt(111) peak and a shift towards higher diffraction angles can be observed (Fig. 3a). The latter clearly indicates Fe-Pt intermixing with the formation of a Pt-rich disordered face-centered cubic (fcc) solid solution. Comparison with SIMS and EDS concentration depth profiles, which will be discussed later, allowed us to conclude that this solution is close to the $FePt_3$ composition. In contrast, annealing of the Au containing sample results in a much broader and more asymmetric (111) reflection already after annealing at 400 °C for 0.5 h (Fig. 3b). Increase of the annealing time up to 2 h leads to the appearance of an additional (111)

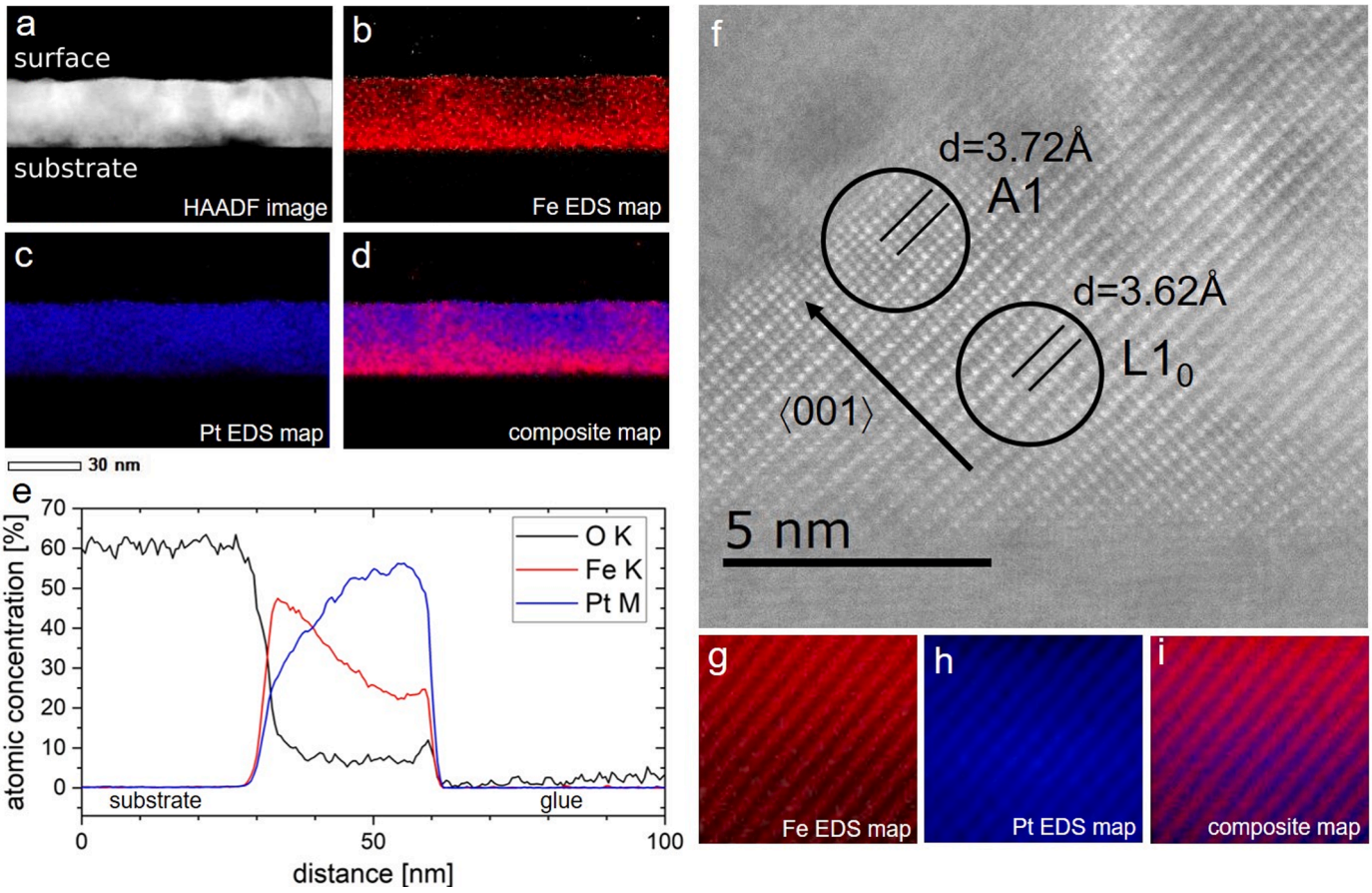

Fig. 6. STEM-EDS analysis of a Fe/Pt bilayer annealed at 450°C for 1 h. (a) HAADF image, (b) Fe and (c) Pt elemental distribution maps, and (d) composition map. (e) EDS averaged linescans of the corresponding elemental mappings for Fe, Pt, and O. Please note that the glue was unintentionally removed from the sample. (f) Atomically resolved HAADF image showing a A1 phase region next to a $L1_0$ ordered region revealing different lattice spacings. For the latter region EDS elemental maps of (g) Fe and (h) Pt and (i) its superposition are displayed revealing clearly the alternating monolayers of Fe and Pt in <001> direction of the $L1_0$ structure.

peak next to the (111) reflection from the Pt-rich fcc solid solution. This additional (111) peak is expected to comprise two FePt phase contributions, $A1$(111) and $L1_0$(111), with almost equiatomic concentration. The presence of the chemically ordered $L1_0$-FePt phase is also confirmed by the occurrence of the (001) $L1_0$-FePt superstructure reflection.

Interestingly, a very similar XRD pattern was found for the Pt/Fe bilayer but after annealing at higher temperatures of 450 °C for 0.5 h (Fig. 4a). Thus, it can be concluded that the introduction of an additional Au layer allows to reduce both the onset temperature and the annealing time needed to promote diffusion-driven phase formation in comparison to Pt/Fe bilayers.

In Fig. 4b XRD patterns of the Pt/Fe/Pt/Au/Fe sample after annealing at 450 °C for different annealing times are displayed. Here, a clear redistribution of the phase composition, expressed by the change of the two (111) peak intensities with increasing annealing time, was observed, which confirms the more pronounced formation of the $A1$/$L1_0$-FePt phase for the sample with Au addition.

As can be seen in the SIMS chemical depth profiles presented in Fig. 5a, annealing of the Pt/Fe bilayer at 450 °C for 0.5 h leads to strong Fe-Pt intermixing throughout the film thickness with an increased Fe signal at the free film surface and reduced Pt content towards the initial Pt/Fe interface. Please note that the enhanced Fe signal at the free surface could be also caused by the presence of Fe oxide since SIMS is highly sensitive to the interatomic interaction and chemical bonding energy [21]. However, additional STEM-EDS analysis confirmed the segregation of Fe to the top surface, as will be discussed later.

A similar structure following the same trend is also detected for the Pt/Fe/Pt/Au/Fe layer stack under these conditions revealing areas with higher (lower) and lower (higher) content of Fe (Pt). In addition, strong Au segregation towards the film/substrate interface is observed (Fig. 5b). It should be noted that the strong overlap of the Au signal with Fe and Si does not necessarily mean that an Fe-Au-Si alloy has formed at this interface as strong chemical roughness could have been developed during the annealing process. For both Pt/Fe and Pt/Fe/Pt/Au/Fe films an increase in annealing time of 1 h leads to a better homogeneity of the elemental distribution (Fig. 5c,d). However, annealing up to 2 h does not show any further change of the elemental distribution (Fig. 5e,f) but promotes the $L1_0$ phase formation, as observed by XRD (Fig. 4).

In order to identify the presence of the different diffusion areas of the Pt/Fe and Pt/Fe/Pt/Au/Fe film samples annealed at 450 °C for 1 h, a

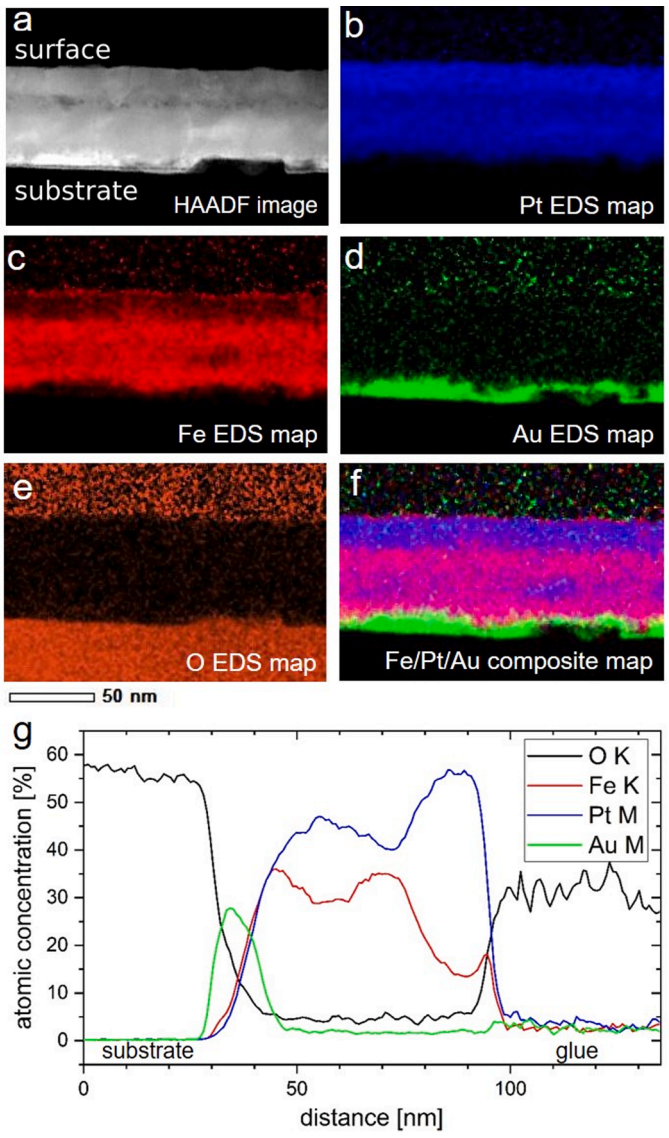

Fig. 7. EDS analysis of the Pt/Fe/Pt/Au/Fe film annealed at 450°C for 1 h. (a) HAADF image with (b) Pt, (c) Fe, (d) Au, and (e) O elemental maps. (f) Composition map. (g) EDS averaged linescans of the corresponding elemental mappings for Fe, Pt, Au, and O.

STEM/EDS analysis of the structure was carried out. Elemental EDS maps of Fe and Pt of the annealed Fe/Pt bilayer are displayed in Fig. 6b and 6c, respectively, showing a strongly intermixed film with a more Pt-rich FePt area closer to the sample surface (Fig. 6d), following the initial layer stacking. From the concentration depth profiles presented in Fig. 6e, a Pt-rich alloy with a Pt:Fe ratio of about 3:1 near the surface region is obtained while the FePt alloy becomes gradually more Fe-rich towards the substrate. Please note that these linescanes are averaged over the full area of the elemental maps shown in Fig. 6b,c. The oxygen concentration was also investigated, which is dominantly present in the substrate (SiO_2) and in the glue. However, an increased O concentration is clearly detected at the film surface, revealing along with the Fe signal the formation of a thin Fe oxide layer. Please note that in this sample the glue got unintentionally removed during sample installation. Furthermore, we performed HAADF imaging with atomic resolution to search in particular for $L1_0(001)$ ordered regions. A corresponding HAADF image is presented in Fig. 6f showing two coexisting phases next to each other with a chemically disordered $A1$ and a chemically ordered $L1_0$ structure. The latter is characterized by alternating monoatomic Fe and Pt planes along the <001> direction of the $L1_0$ structure, as shown by the high resolution elemental maps of Fig. 6g-i.

For the annealed Pt/Fe/Pt/Au/Fe layer stack, first an oxidized Fe surface layer is clearly seen in the corresponding elemental maps and EDS averaged linescanes displayed in Fig. 7, then a Pt-rich FePt area is present near the surface region followed by an intermixed FePt region and again by a more Pt-rich FePt area (close to $FePt_3$). However, the Au layer has rearranged in position and is now fully located next to the substrate interface (Fig. 7d-g) without containing noticeable traces of Pt or Fe, which is on a first glance in contradiction to the SIMS results. However, in this case the chemical roughness which has developed during the annealing process is too severe and thus results in overlapping signals of the elements as the signals in the SIMS experiments are averaged and collected over an area of 96.4 μm x 96.4 μm.

The differences in the microstructure as well as the degree of chemical ordering and phase mixing should also be disclosed in the magnetic properties. The room temperature M-H hysteresis loops of the samples in the as-deposited state are presented in Fig. 8a,b. They reveal a soft-magnetic behavior of the Fe layers with an in-plane easy magnetization given by the magnetic shape anisotropy. In contrast, the loops of the samples annealed at 450°C for 1 h display much higher coercive fields and an isotropic behavior when measured along the in-plane and out-of-plane geometry which is expected due to the polycrystalline nature of the samples (Fig. 8c,d). However, the annealed Pt/Fe/Pt/Au/Fe film exhibits a noticeable higher coercive field of about 765 kA/m compared to 605 kA/m, which is consistent with the presence of a higher fraction of the magnetically hard $L1_0$-FePt phase. In addition, a hardening effect due to the incorporation of Au to the FePt grain boundaries resulting in a magnetic decoupling of the FePt grains might contribute as well to the coercivity enhancement [22] but is expected to be of minor importance as most of the Au is located at the film substrate interface. As both samples exhibit pronounced hard and soft magnetic phase mixtures, the impact of the graded structure on the coercivity is however difficult to disentangle.

4. Conclusions

Asymmetric Pt/Fe/Pt/Au/Fe layer stacks including an Au layer were magnetron sputtered at room temperature and subjected to post-annealing in vacuum varying the annealing temperature and time. The evolution of their structure and magnetic properties were investigated by a variety of techniques including XRD, SIMS, STEM-EDS, as well as SQUID-VSM magnetometry. These properties were compared with characteristics of post-annealed Pt/Fe bilayer thin films. It was shown that the introduction of the Au layer allows to reduce both the onset temperature and the annealing time needed to promote diffusion-driven structural phase transitions in comparison to Pt/Fe bilayers. Furthermore, the introduction of an additional Au layer results in a higher coercive field of a post-annealed Pt/Fe/Pt/Au/Fe stack (765 kA/m) compared to the Pt/Fe bilayer (605 kA/m) caused by the differences in the microstructure as well as the degree of chemical ordering of the thin film material. Employing functional layers of third elements to Fe/Pt stacks which induces different thermally driven diffusion processes is a

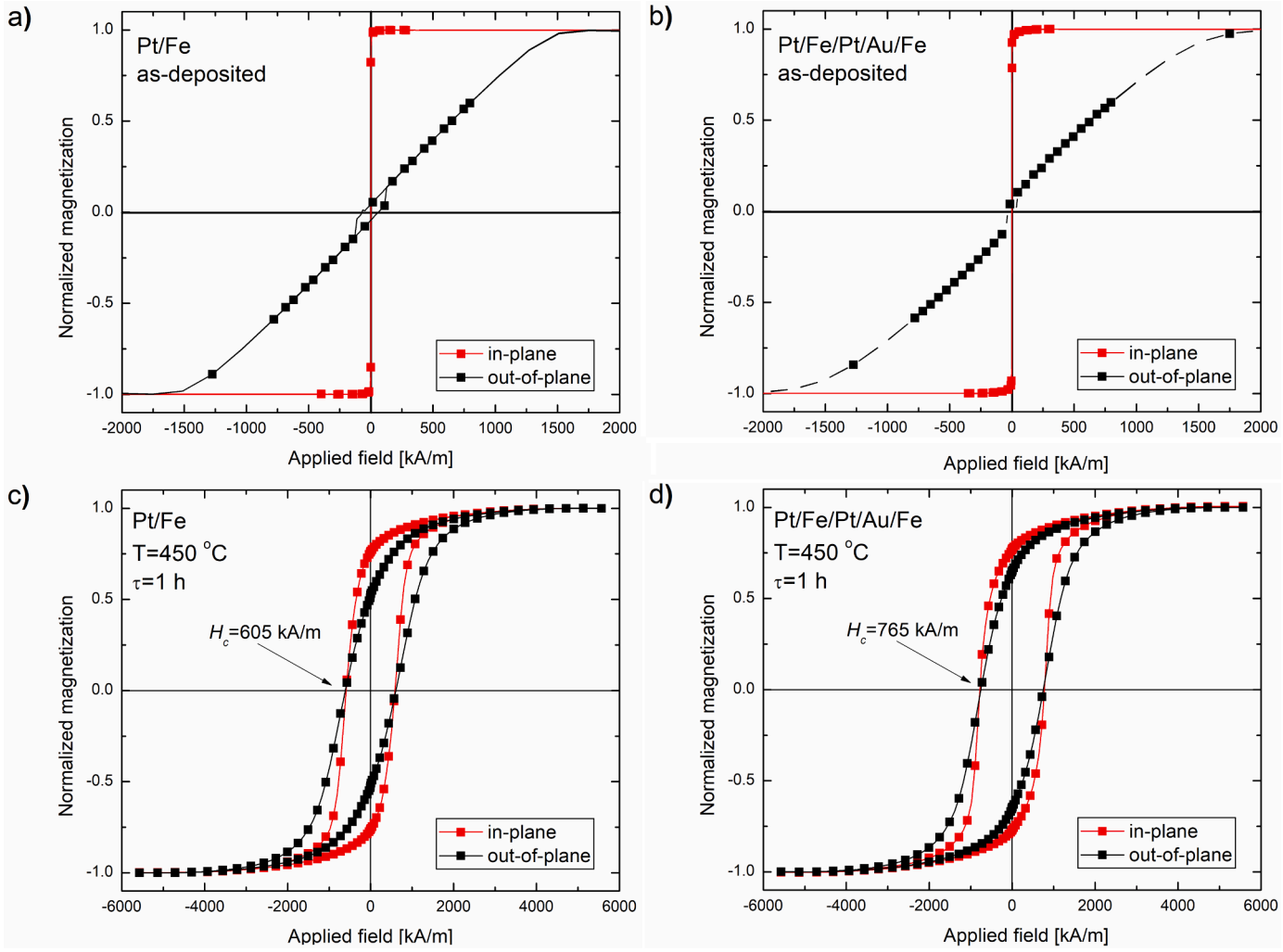

Fig. 8. Room temperature SQUID-VSM (M-H) hysteresis loops of as-deposited (a) Pt/Fe and (b) Pt/Fe/Pt/Au/Fe films and (c, d) after annealing at 450°C for 1 h, respectively.

promising pathway to create in a self-organized way heterostructures consisting of different phases with varying physical properties.

CRediT authorship contribution statement

I.A. Vladymyrskyi: Conceptualization, Investigation, Funding acquisition, Project administration, Writing – original draft, Writing – review & editing. **Y. Mamchur:** Investigation. **O.V. Dubikovskyi:** Investigation. **S.M. Voloshko:** Investigation. **A. Ullrich:** Investigation. **M. Albrecht:** Funding acquisition, Project administration, Writing – review & editing.

Declaration of Competing Interest

None.

Acknowledgment

This work was financially supported by the Deutsche Forschungsgemeinschaft (DFG, German Research Foundation) – project number 370878165 and by the Ministry of Education and Science of Ukraine – project number 0119U001483.

References

[1] I. Suzuki, S. Kubo, H. Sepehri-Amin, Y.K. Takahashi, Dependence of the growth mode in epitaxial FePt films on surface free energy, ACS Appl. Mater. Interfaces 13 (2021) 16620, https://doi.org/10.1021/acsami.0c22510.
[2] I. Suzuki, J. Wang, Y.K. Takahashi, K. Hono, Control of grain density in FePt-C granular thin films during initial growth, J. Magn. Magn. Mater. 500 (2020), 166418, https://doi.org/10.1016/j.jmmm.2020.166418.
[3] A. Hafarov, O. Prokopenko, S. Sidorenko, D. Makarov, and I. Vladymyrskyi, L10 ordered thin films for spintronic and permanent magnet applications, in A. Kaidatzis, S. Sidorenko, I. Vladymyrskyi, D. Niarchos (eds) Modern Magnetic and Spintronic Materials. NATO Science for Peace and Security Series B: Physics and Biophysics. Springer, Dordrecht. (2020) 73, https://doi.org/10.1007/978-94-024-2034-0_4.
[4] L. Zhang, K. Han, X. Zhang, E. Wang, J. Lu, R. Goddard, Effect of a high magnetic field on hard magnetic multilayered Fe-Pt alloys, J. Magn. Magn. Mater. 490 (2019), 165533, https://doi.org/10.1016/j.jmmm.2019.165533.
[5] S. Maenosono, S. Saita, Theoretical assessment of FePt nanoparticles as heating elements for magnetic hyperthermia, IEEE Trans. Magn. 42 (2006) 1638, https://doi.org/10.1109/TMAG.2006.872198.
[6] L. Liu, H. Lv, W. Sheng, Y. Lou, J. Bai, J. Cao, B. Ma, F. Wei, Orientation control in L10 FePt films by using magnetic field annealing around Curie temperature, Appl. Surf. Sci. 258 (2012) 5770, https://doi.org/10.1016/j.apsusc.2012.02.090.
[7] F.M.F. Rhen, G. Hinds, C. O'Reilly, J.M.D. Coey, Electrodeposited FePt films, IEEE Trans. Magn. 39 (2003) 2699, https://doi.org/10.1109/TMAG.2003.815566.
[8] D.P. Nguyen, S.-Y. O, C.W. Park, K. Shin, C.-G. Lee, T. Shimozaki, T. Okino, The effect of thickness and annealing condition on the microstructure and magnetic properties of Fe/Pt multilayer thin films, J. Magn. Magn. Mater. 320 (2008) e264, https://doi.org/10.1016/j.jmmm.2008.02.176.
[9] B. Yao, K.R. Coffey, The influence of periodicity on the structures and properties of annealed [Fe/Pt]n multilayer films, J. Magn. Magn. Mater. 320 (2008) 559, https://doi.org/10.1016/j.jmmm.2007.07.030.

[10] C. Feng, B.H. Li, G. Han, J. Teng, Y. Jiang, T. Yang, G.H. Yu, Effect of the underlayer (Ag, Ti or Bi) on the magnetic properties of Fe/Pt multilayer films, Thin Solid Films 515 (2007) 8009, https://doi.org/10.1016/j.tsf.2007.03.181.
[11] I.O. Kruhlov, O.V. Shamis, N.Y. Schmidt, M.V. Karpets, S. Gulyas, E. Hadjixenophontos, A.P. Burmak, S.I. Sidorenko, G.L. Katona, G. Schmitz, M. Albrecht, I.A. Vladymyrskyi, Structural phase transformations in annealed Pt/Mn/Fe trilayers, J. Phys.: Condens. Matter 32 (2020), 365404, https://doi.org/10.1088/1361-648X/ab9269.
[12] I.O. Kruhlov, O.V. Shamis, N.Y. Schmidt, S. Gulyas, R. Lawitzki, A.P. Burmak, S. I. Konorev, G.L. Katona, G. Schmitz, M. Albrecht, I.A. Vladymyrskyi, Thermally-induced phase transitions in Pt/Tb/Fe trilayers, Thin Solid Films 709 (2020), 138134, https://doi.org/10.1016/j.tsf.2020.138134.
[13] Y. Ogata, Y. Imai, S. Nakagawa, Effect of third element for FePt ordered alloy thin films with perpendicular magnetic anisotropy fabricated from Fe/Pt/X trilayer, Phys. Procedia 16 (2011) 36, https://doi.org/10.1016/j.phpro.2011.06.104.
[14] Y.S. Yu, H.-B. Li, W.L. Li, M. Liu, Y.-M. Zhang, W.D. Fei, Structure and magnetic properties of magnetron-sputtered [(Fe/Pt/Fe)/Au]n multilayer films, J. Magn. Magn. Mater. 322 (2010) 1770, https://doi.org/10.1016/j.jmmm.2009.12.027.
[15] I.A. Vladymyrskyi, A.E. Gafarov, A.P. Burmak, S.I. Sidorenko, G.L. Katona, N. Y. Safonova, F. Ganss, G. Beddies, M. Albrecht, Yu.N. Makogon, D.L. Beke, Low-temperature formation of the FePt phase in the presence of an intermediate Au layer in Pt /Au /Fe thin films, J. Phys. D: Appl. Phys. 49 (2016), 035003, https://doi.org/10.1088/0022-3727/49/3/035003.
[16] L. Fallarino, B.J. Kirby, E.E. Fullerton, Graded magnetic materials, J. Phys. D: Appl. Phys. 54 (2021), 303002, https://doi.org/10.1088/1361-6463/abfad3.
[17] C.-C. Chiang, W.-C. Tsai, L.-W. Wang, H.-C. Hou, J.-W. Liao, H.-J. Lin, F.-H. Chang, B.J. Kirby, C.-H. Lai, (001) FePt graded media with PtMn underlayers, Appl. Phys. Lett. 99 (2011), 212504, https://doi.org/10.1063/1.3664129.
[18] D. Goll, A. Breitling, L. Gu, P.A. van Aken, W. Sigle, Experimental realization of graded 10-FePt/Fe composite media with perpendicular magnetization, J. Appl. Phys. 104 (2008), 083903, https://doi.org/10.1063/1.2999337.
[19] F. Wang, J. Zhang, J. Zhang, C. Wang, Z. Wang, H. Zeng, M. Zhang, X. Xu, Graded/soft/graded exchange-coupled thin films fabricated by [FePt/C]5/Fe/[C/FePt]5 multilayer deposition and post-annealing, Appl. Surf. Sci. 271 (2013) 390, https://doi.org/10.1016/j.apsusc.2013.01.211.
[20] D. Mitin, M. Wachs, N.Y. Safonova, O. Klein, M. Albrecht, Exchange coupled L10 FeCuPt/Fe heterostructures: Magnetic properties and reversal behavior at elevated temperatures, Thin Solid Films 651 (2018) 158, https://doi.org/10.1016/j.tsf.2017.06.059.
[21] V. Cherepin, Secondary Ion Mass Spectroscopy of Solid Surfaces, VNW Science Press, Ultrecht, the Netherlands, 1987, https://doi.org/10.1201/9780429070327.
[22] F.T. Yuan, S.K. Chen, W.M. Liao, C.W. Hsu, S.N. Hsiao, W.C. Chang, Very high coercivities of top-layer diffusion Au/FePt thin films, J. Magn. Magn. Mater. 304 (2006) e109, https://doi.org/10.1016/j.jmmm.2006.01.194.